J. Austral. Math. Soc. Ser. B 25 (1983), 190–216

A DISCRETE FOURIER ANALYSIS OF COARSE MESH REBALANCING AND SOME ASSOCIATED ITERATIVE METHODS

J. M. BARRY[1], J. H. JENKINSON[2] and J. P. POLLARD[1]

(Received 29 June 1982; revised 9 November 1982)

Abstract

Iterative methods for solving systems of linear equations may be accelerated by coarse mesh rebalance techniques. The iterative technique, the Method of Implicit Non-stationary Iteration (MINI), is examined through a local-mode Fourier analysis and compared to relaxation techniques as a potential candidate for such acceleration. Results of a global-mode Fourier analysis for MINI, relaxation methods, and the conjugate gradient method are reported for two test problems.

1. Introduction

The finite difference (or finite element) approximation to many problems of mathematical physics requires the efficient solution of large sparse systems of linear equations. While direct solution techniques are attractive for solving $A\mathbf{x} = \mathbf{b}$ in many practical cases (particularly now that large computational facilities are available), the iterative techniques remain the most promising means of solving the extremely large systems of linear equations that arise in many applications. This is particularly true in neutron diffusion studies where equations of the order 10^5 are commonplace.

One recently devised iterative technique, the Method of Implicit Non-stationary Iteration (MINI) (Barry and Pollard [2, 3, 4]) has undergone considerable testing and use with the three-dimensional nuclear code POW3D (Barry, Harrington and Pollard [1]). The method essentially uses an implicit estimate on each

[1] Australian Atomic Energy Commission, Lucas Heights Research Laboratories, Private Mail Bag, Sutherland, N.S.W. 2232.

[2] Department of Mathematics, Australian National University, P.O. Box 4, Canberra, A.C.T. 2600.

iterative pass to update the solution at all points of the grid not yet updated.

In a point form the Gauss-Seidel iterative scheme

$$\sum_{j<i} a_{ij}x_j^{(n+1)} + a_{ii}x_i^{(n+1)} + \sum_{j>i} a_{ij}x_j^{(n)} = b_i,$$

improves upon the Jacobi method by using all the latest information available to it. MINI seeks to improve upon the Gauss-Seidel method by improving the terms associated with the nth pass with an implicit weighted correction determined from the increment to the ith unknown; as yet undetermined. A point version of MINI is

$$\sum_{j<i} a_{ij}x_j^{(n+1)} + a_{ii}x_i^{(n+1)} + \sum_{j>i} a_{ij}\left(x_j^{(n)} + \gamma_{ij}^{(n)}\left(x_i^{(n+1)} - x_i^{(n)}\right)\right) = b_i. \quad (1.1)$$

The weighting factors $\gamma_{ij}^{(n)}$ are determined through an algorithm outlined by Barry and Pollard [2], and may change on each iterative pass. Suffice it to say at this stage, each $\gamma_{ij}^{(n)}$ is subject to the restriction $0 \leqslant \gamma_{ij}^{(n)} \leqslant 1$. This was found to be essential when MINI was formulated for specific application in neutron diffusion studies, where a positive solution is essential. Like all relaxation schemes MINI can be used in a block form, and the improved convergence performance anticipated is realised.

Unlike the more traditional iterative methods such as successive over-relaxation (SOR), where considerable accumulated knowledge exists (Varga [19] and Young [21]), little is known about MINI. All iterative methods, however, are known to decrease error in estimates of the solution in proportion to the absolute magnitude of each eigenvalue, when the error is expanded in terms of the eigenvectors of the iteration matrix. This expansion has limited use in studies of error removal because the eigenvectors and eigenvalues can be specified directly for only the simplest forms of differential operators.

It has been traditional in reactor physics (following Wachspress [20]) to use variational acceleration techniques and so hasten convergence of the ordinary iterative process. Methods such as SOK (Pollard [16]) are employed along with more sophisticated 'finite element like' approximations reported by Nakamura [11–14].

This process of effective acceleration, known eventually as coarse mesh rebalancing, remained largely ignored outside reactor physics until recently, and still lacks a solid mathematical backing. One justification for its success is based on the assumption that, for a particular iteration matrix, the geometric frequencies of the eigenvectors and the magnitude of the eigenvalues are inversely related; Nakamura [14] established that coarse mesh rebalancing for a particular choice of weighting vectors completely removes the low eigenvector components of error from the solution estimate. Unfortunately these weighting vectors are the eigenvectors of the iteration matrix and so are unavailable in practical situations.

Nevertheless, somewhat arbitrary correction vectors, computed on a coarse mesh, and with even trivial weighting vectors, are well known to be a worthwhile way of accelerating the fine mesh iterations.

In a more recent approach, Brandt [6] describes a multigrid scheme for hastening the rate of convergence for several iterative methods. This approach rests on the assertion that the fine mesh iterative scheme rapidly reduces the high frequency error components in the solution estimate (and the hope that the more difficult low frequency components can be removed by iterating over a series of grids of increasing coarseness when difficulty in convergence on the fine grid is observed). Support for this assertion is based on what Brandt [6] and Nicolaides [15] describe as a 'local mode' error analysis of some iterative approaches.

In this analysis a smoothing factor $\mu(\theta)$ is used as a measure of the decay induced in each Fourier component of the error by an iterative step. The analysis is performed at a single grid point far removed from the boundary. A similar analysis is given here for the point version of MINI. Smoothing factors for other schemes are quoted and compared. Brandt's approach is somewhat artificial in that it distorts the structure of the actual matrix involved by ignoring the boundary conditions. Although the local mode analysis technique comes in for some mathematical criticism as to its general applicability, the insight and agreement with other analyses of error it provides are sufficient justification to report on it here.

Four methods of coarse mesh rebalancing are subjected to a Fourier analysis in this work. The four methods form part of the support system for the nuclear code POW3D, where they have been extensively tested on real reactor configurations. These reactor calculations led to the conclusions that, at worst, coarse mesh rebalancing does not penalise the working of the code, the solution time for most reactor models is shortened, and, for more difficult reactor configurations, some form of coarse mesh rebalancing is essential.

2. A 'local mode' Fourier analysis

Consider a general equation of the form

$$-a\frac{\partial^2 u}{\partial x^2} - b\frac{\partial^2 u}{\partial y^2} = F(x, y), \tag{2.1}$$

subject to appropriate Dirichlet or Neumann boundary conditions. This equation can be approximated at a mesh point with indices (α, β) situated away from the

boundary by the following finite difference representation:

$$a(-U_{\alpha+1\,\beta} + 2U_{\alpha\,\beta} - U_{\alpha-1\,\beta}) + b(-U_{\alpha\,\beta+1} + 2U_{\alpha\,\beta} - U_{\alpha\,\beta-1}) = h^2 F_{\alpha\,\beta}, \tag{2.2}$$

where an evenly spaced mesh of width h is assumed about (α, β).

Let $\mathbf{u}$ and $\bar{\mathbf{u}}$ represent the (n) and $(n+1)$ iterate approximations respectively for U during a MINI iteration, where the solution procedure already has passed through the points $(\alpha, \beta - 1)$ and $(\alpha - 1, \beta)$. Applying MINI to the form given in equation (2.2) (and, for convenience, dropping the iteration dependence of γ) gives

$$\begin{aligned} &a\big(-u_{\alpha+1\,\beta} - \gamma_{\alpha+1\,\beta}(\bar{u}_{\alpha\,\beta} - u_{\alpha\,\beta}) + 2\bar{u}_{\alpha\,\beta} - \bar{u}_{\alpha-1\,\beta}\big) \\ &\quad + b\big(-u_{\alpha\,\beta+1} - \gamma_{\alpha\,\beta+1}(\bar{u}_{\alpha\,\beta} - u_{\alpha\,\beta}) + 2\bar{u}_{\alpha\,\beta} - \bar{u}_{\alpha\,\beta-1}\big) = h^2 F_{\alpha\,\beta}. \end{aligned} \tag{2.3}$$

The finite difference approximation (2.2) may be altered by the inclusion of two zero terms $\gamma_{\alpha+1\,\beta}(U_{\alpha\,\beta} - U_{\alpha\,\beta})$ and $\gamma_{\alpha\,\beta+1}(U_{\alpha\,\beta} - U_{\alpha\,\beta})$ respectively to

$$\begin{aligned} &a\big(-U_{\alpha+1\,\beta} - \gamma_{\alpha+1\,\beta}(U_{\alpha\,\beta} - U_{\alpha\,\beta}) + 2U_{\alpha\,\beta} - U_{\alpha-1\,\beta}\big) \\ &\quad + b\big(-U_{\alpha\,\beta+1} - \gamma_{\alpha\,\beta+1}(U_{\alpha\,\beta} - U_{\alpha\,\beta}) + 2U_{\alpha\,\beta} - U_{\alpha\,\beta-1}\big) = h^2 F_{\alpha\,\beta}. \end{aligned} \tag{2.4}$$

Let the error between the solution $\mathbf{U}$ and the two subsequent iterates $\mathbf{u}$ and $\bar{\mathbf{u}}$ be written as

$$\mathbf{v} = \mathbf{U} - \mathbf{u}$$

and

$$\bar{\mathbf{v}} = \mathbf{U} - \bar{\mathbf{u}}.$$

Subtracting equation (2.3) from equation (2.4) gives

$$\begin{aligned} &a\big(-v_{\alpha+1\,\beta} - \gamma_{\alpha+1\,\beta}(\bar{v}_{\alpha\,\beta} - v_{\alpha\,\beta}) + 2\bar{v}_{\alpha\,\beta} - \bar{v}_{\alpha-1\,\beta}\big) \\ &\quad + b\big(-v_{\alpha\,\beta+1} - \gamma_{\alpha\,\beta+1}(\bar{v}_{\alpha\,\beta} - v_{\alpha\,\beta}) + 2\bar{v}_{\alpha\,\beta} - \bar{v}_{\alpha\,\beta-1}\big) = 0 \end{aligned} \tag{2.5}$$

as an expression of error about the point (α, β).

The γs are assumed to be constant in any direction (that is positionally independent) for the following analysis. (In normal practice this is not generally the situation and so the analysis is necessarily restrictive). Consequently $\gamma_{\alpha+1\,\beta}$ and $\gamma_{\alpha\,\beta+1}$ are written as γ_x and γ_y respectively to indicate the independence. Now, in a Fourier study, the (θ_1, θ_2) components of the error vectors on subsequent iterations are

$$v_{\alpha\,\beta} = \sum_{\theta_1} \sum_{\theta_2} A_{\theta_1\theta_2} e^{i(\alpha\theta_1 + \beta\theta_2)}$$

and

$$\bar{v}_{\alpha\,\beta} = \sum_{\theta_1} \sum_{\theta_2} \bar{A}_{\theta_1\theta_2} e^{i(\alpha\theta_1 + \beta\theta_2)}.$$

https://doi.org/10.1017/S033427000000401X Published online by Cambridge University Press

Substitution into the linear relation (2.5) and use of the linear independence of the Fourier vectors to separate coefficients yields

$$\bar{A}_{\theta_1\theta_2}\left(-a\gamma_x + 2a - b\gamma_y + 2b - ae^{-i\theta_1} - be^{-i\theta_2}\right) + A_{\theta_1\theta_2}\left(-ae^{i\theta_1} + a\gamma_x - be^{i\theta_2} + b\gamma_y\right) = 0,$$

for all θ_1 and θ_2.

A smoothing coefficient (or damping factor) $\mu(\theta_1, \theta_2)$ is introduced to measure the damping effect on a particular Fourier term after one iteration. It is defined as the ratio of the absolute magnitude of the Fourier coefficients after an iteration to those before, *i.e.*

$$\mu(\theta_1, \theta_2) = \frac{|\bar{A}_{\theta_1\theta_2}|}{|A_{\theta_1\theta_2}|}.$$

For the point version of MINI

$$\mu_{\text{MINI}}(\theta_1, \theta_2) = \frac{|ae^{i\theta_1} + be^{i\theta_2} - a\gamma_x - b\gamma_y|}{|2a + 2b - a\gamma_x - b\gamma_y - ae^{-i\theta_1} - be^{-i\theta_2}|}. \tag{2.6}$$

Note that this 'local mode' error analysis is for the five point linear relation (2.5) and not the full MINI iterative process (1.1). This form of analysis is capable only of giving some idea of what might happen to the error components at mesh points away from the boundary. For most reactor systems the grids are relatively fine, so the majority of points fit into this category. Any attempt to extend the explanation to the full process encounters problems that are identified in the following treatment (Doherty [8]).

Consider the linear system

$$A\mathbf{u} = \mathbf{s}$$

with the following splitting of A

$$A = M - N,$$

which allows the linear system to be expressed

$$M\mathbf{u} = N\mathbf{u} + \mathbf{s}. \tag{2.7}$$

This leads to the iterative scheme

$$\mathbf{u}^{(n+1)} = M^{-1}N\mathbf{u}^{(n)} + M^{-1}\mathbf{s}. \tag{2.8}$$

Subtracting (2.7) from (2.8) yields

$$\mathbf{u}^{(n+1)} - \mathbf{u} = M^{-1}N(\mathbf{u}^{(n)} - \mathbf{u}). \tag{2.9}$$

https://doi.org/10.1017/S033427000000401X Published online by Cambridge University Press

Assuming the completeness of the set of eigenvectors $\mathbf{w}_i$ of $M^{-1}N$ the error vector at step $(n+1)$ may be expanded

$$(\mathbf{u}^{(n)} - \mathbf{u}) = \sum_i a_i^{(n)} \mathbf{w}_i$$

or

$$(\mathbf{u}^{(n)} - \mathbf{u}) = W\mathbf{a}^{(n)},$$

where W is a (square) matrix whose columns are the eigenvectors $\mathbf{w}_i$, and the components of $\mathbf{a}^{(n)}$ are the coefficients of the error expansion. Then

$$\mathbf{a}^{(n)} = W^{-1}(\mathbf{u}^{(n)} - \mathbf{u})$$

and hence

$$\begin{aligned} \mathbf{a}^{(n+1)} &= W^{-1}(\mathbf{u}^{(n+1)} - \mathbf{u}) \\ &= W^{-1}M^{-1}N(\mathbf{u}^{(n)} - \mathbf{u}) \\ &= W^{-1}M^{-1}NW\mathbf{a}^{(n)} = T\mathbf{a}^{(n)}. \end{aligned} \tag{2.10}$$

Here, T is a diagonal matrix whose elements are the eigenvalues of the matrix. Under these conditions, it seems natural to analyse the iterative technique in terms of the coefficients of the eigenvector expansion of error. For the simple case of $\mathbf{a}$ and $\mathbf{b}$ constant in (2.2), the orthogonal eigenvectors of the Jacobi scheme are the Fourier terms, and the local mode analysis is justified rigorously. For more complex elliptical systems, the completeness of the set of eigenvectors is no longer assured, nor is it clear that for MINI the analysis could have been applied due to the uncertainty about the eigenvectors of the iteration matrix. Consequently, the separation of error components, as performed in the point analysis (2.6), cannot be rigorously justified by an analysis of the iterative scheme, although there is ample empirical evidence of its success. The approach is pursued, however, for the insights it provides into the various iterative schemes.

The smoothing factor for SOR with relaxation parameter ω may be found similarly to the way in which (2.6) was derived for MINI (Barry [5]).

$$\mu_{\mathrm{SOR}}(\theta_1, \theta_2) = \frac{|ae^{i\theta_1} + be^{i\theta_2} - 2a(\omega - 1)/\omega - 2b(\omega - 1)/\omega|}{|2a/\omega + 2b/\omega - ae^{-i\theta_1} - be^{-i\theta_2}|}. \tag{2.11}$$

Consideration of a formal connection between point MINI and SOR (Barry and Pollard [2]) demonstrates the necessary degree of equivalence between (2.6) and (2.11). Point methods, however, are seldom used in fine mesh calculations because the rate of convergence is inferior to block or line versions. For two-dimensional problems, a line version of MINI (LMINI) (Barry and Pollard [3]) or SOR (SLOR) generally solves along each mesh line in turn. This requires the solution of a tridiagonal system of linear equations. For three-dimensional problems, such

https://doi.org/10.1017/S033427000000401X Published online by Cambridge University Press

as those tackled by the nuclear code POW3D (Barry, Harrington and Pollard [1]), the blocking is usually in terms of (x, y) planes, which in turn are solved by line techniques (LMINI or SLOR).

The way in which the smoothing factors for the line and block oriented schemes are obtained is similar to that for point methods, (Barry [5]). The smoothing factors for LMINI and SLOR with lines taken parallel to the x-axis are given by

$$\mu_{\text{LMINI}}(\theta_1, \theta_2) = \frac{|be^{i\theta_2} - b\gamma_y|}{|2a + 2b - b\gamma_y - ae^{i\theta_1} - ae^{-i\theta_1} - be^{-i\theta_2}|}, \tag{2.12}$$

and

$$\mu_{\text{SLOR}}(\theta_1, \theta_2) = \frac{\left|\frac{a(\omega-1)}{\omega}[e^{i\theta_1} - 2 + e^{-i\theta_1}] + be^{i\theta_2} - \frac{2b(\omega-1)}{\omega}\right|}{\left|\frac{a}{\omega}[e^{i\theta_1} - 2 + e^{-i\theta_1}] - \frac{2b}{\omega} + be^{-i\theta_2}\right|}, \tag{2.13}$$

respectively. For the three-dimensional analogue of (2.1),

$$-a\frac{\partial^2 u}{\partial x^2} - b\frac{\partial^2 u}{\partial y^2} - c\frac{\partial^2 u}{\partial z^2} = F(x, y, z), \tag{2.14}$$

the block forms of MINI (BMINI) and SOR (SBOR) have the following smoothing factors provided the plane iterations are converged

$$\mu_{\text{BMINI}}(\theta_1, \theta_2, \theta_3) = \frac{|ce^{i\theta_3} - c\gamma_z|}{|2a + 2b + 2c - c\gamma_z - ae^{-i\theta_1} - be^{-i\theta_2} - ae^{i\theta_1} - be^{i\theta_2} - ce^{-i\theta_3}|}, \tag{2.15}$$

and

$$\mu_{\text{SBOR}}(\theta_1, \theta_2, \theta_3) = \frac{|ap[e^{i\theta_1} - 2 + e^{-i\theta_1}] + bp[e^{i\theta_2} - 2 + e^{-i\theta_2}] + ce^{i\theta_3} - 2cp|}{\left|\frac{a}{\omega}[e^{i\theta_1} - 2 + e^{-i\theta_1}] + \frac{b}{\omega}[e^{i\theta_2} - 2 + e^{-i\theta_2}] - \frac{2c}{\omega} + ce^{-i\theta_3}\right|}, \tag{2.16}$$

where $p = (\omega - 1)/\omega$.

Inspection of (2.6), (2.11), (2.12), (2.13), (2.15) and (2.16) reveals, in general, that while θ increases for most a, b (and c) $\mu(\theta)$ decreases and is less than 1. (No such strong smoothing is indicated for the six schemes when θ is small; in fact as $\theta \to 0$, $\mu(\theta) \to 1$.)

https://doi.org/10.1017/S033427000000401X Published online by Cambridge University Press

There are some minor violations of this phenomenon of smoothing, such as occur with point MINI, where $\mu(\theta)$ is also dependent upon γ. For the case of any a, b, and θ for $\gamma = 1$,

$$\mu_{\text{MINI}}(\theta_1, \theta_2) = \frac{|ae^{i\theta_1} + be^{i\theta_2} - a - b|}{|ae^{-i\theta_1} + be^{-i\theta_2} - a - b|} = 1.$$

The result is no reduction for any of the error component frequencies. Fortunately with MINI, although $\gamma = 1$ is permitted, it is a value that arises infrequently in practice, and because it is recalculated after every iteration the probability of its persistence is even lower. The same behaviour is observed for SOR, SLOR and SBOR as $\omega \to 2$. Brandt [6] notes the Gauss-Seidel case for $a \ll b$, where $\mu(\pi/2, 0) \to 1$ as $a \to 0$. An appropriately oriented line version, however, overcomes this shortcoming of the point iterative approach, as consideration of (2.13) reveals.

In Figure 1 the smoothing factor is plotted as a function of γ and ω for the highest frequency component of error with point MINI and SOR methods. The results are shown for the operator $-\nabla^2$ on a 16×16 finite difference grid over a square region of side length π. Both point and line methods are displayed, and the expected advantage of the line approach is realised. Although not immediately obvious from Figure 1, MINI and SOR are equivalent if $\omega = 2/(2 - \gamma)$. For the line version, the superiority of MINI appears more marked. This is predicted from the point theory (Barry and Pollard [2]). No such simple theoretical relationship exists for the line or block versions of the two methods (Barry [5]).

An examination of MINI (2.6) with the local mode approach reveals that no smoothing occurs for $\gamma > 1$. This supports the upper restriction placed on γ for MINI (discussed in Section 1) and found to be desirable in practice. The theoretical upper bound on ω for SOR is suggested similarly by the smoothing factor (2.11).

The smoothing factor $\mu(\theta_1, \theta_2)$ (with θ_1 and θ_2 again chosen equal) is plotted once more for the same operator equation in Figure 2. This time three different frequency components are shown as functions of γ for point MINI and LMINI. The components chosen represent low ($\theta_1 = \pi/15$), middle ($\theta_7 = 7\pi/15$) and high ($\theta_{14} = 14\pi/15$) frequency divisions of the spectrum. The comparison suggests that the high frequencies will be removed more quickly by the iterative scheme, and that the lower ones will persist. The smoothing factors for SOR and SLOR (calculated with the optimal ω in each case) are superimposed in the figure for the same frequency components. There appears to be little difference between point MINI and SOR for the lower frequencies, but at higher frequencies the differences are more marked for a large portion of the range of admissible γs. For the line version of MINI, this tendency is even more pronounced. The greatest

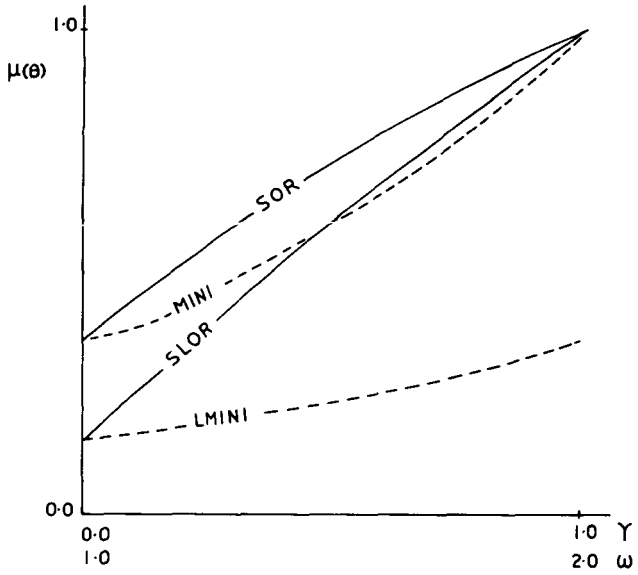

FIGURE 1. Smoothing factor as a function of γ and ω for the high frequency error component ($\theta = 14\pi/15$) of the operator $-(\partial^2 u/\partial x^2 + \partial^2 u/\partial y^2)$ on a square region of side π.

smoothing for the low frequency error of MINI coincides with the corresponding smoothing factor for optimal SOR. The graph demonstrates that, for this particular value of γ, the other high smoothing components for MINI also coincide with the optimal SOR smoothing factor. For line MINI and SLOR, a similar coincidence is suggested for low frequency error but is not repeated for high frequency error, not a surprising outcome because there is no such simple equivalence between the line versions.

The results show conclusively that MINI handles the high frequency error terms more efficiently than it does the lower components.

Examination of (2.15) and a three-dimensional analogue of (2.6) suggests that the block form of MINI is more smoothing than point MINI for the three-dimensional problem. A similar examination of (2.13) and (2.11) supports the same suggestion for line MINI over point MINI for the two-dimensional problem. When MINI was introduced in the nuclear code, the block forms were expected to have a higher rate of convergence. In the absence of a formal analysis of the convergence of MINI, this expectation based on local mode analysis is reassuring.

In Figure 3 the smoothing factor is shown as a function of γ when $\theta = \pi/15$, $5\pi/15$, $7\pi/15$, and $14\pi/15$, for the point and line versions of MINI on a two-dimensional 16×16 grid with the previous operator. In addition, a smoothing factor for the three-dimensional operator (equation (2.13)) is included, where

https://doi.org/10.1017/S033427000000401X Published online by Cambridge University Press

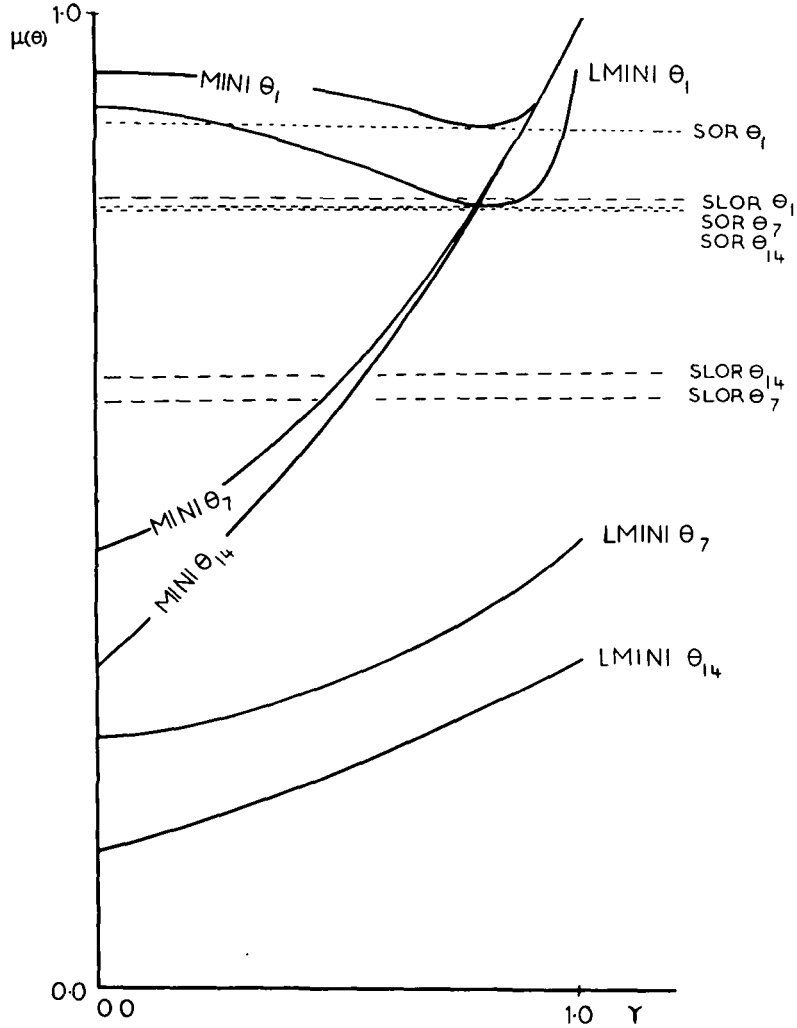

FIGURE 2. Smoothing factor as a function of γ for MINI with the operator $-(\partial^2 u/\partial x^2 + \partial^2 u/\partial y^2)$ for the error component frequencies $\theta_j = j\pi/15$.

the solution process is block MINI, on a $16 \times 16 \times 16$ grid. In Figure 4, a similar situation is displayed for the smoothing factor of the successive over-relaxation forms, shown as a function of ω. The smoothing factors for block MINI and SBOR apply to the outer level (*i.e.* z-direction iterative scheme) for the two-level block process. Figure 3 demonstrates clearly (for all frequencies displayed), that the block MINI process for the third spatial dimension possesses superior smoothing qualities to those of the simpler line or point form on a two-dimensional grid of comparable order.

https://doi.org/10.1017/S033427000000401X Published online by Cambridge University Press

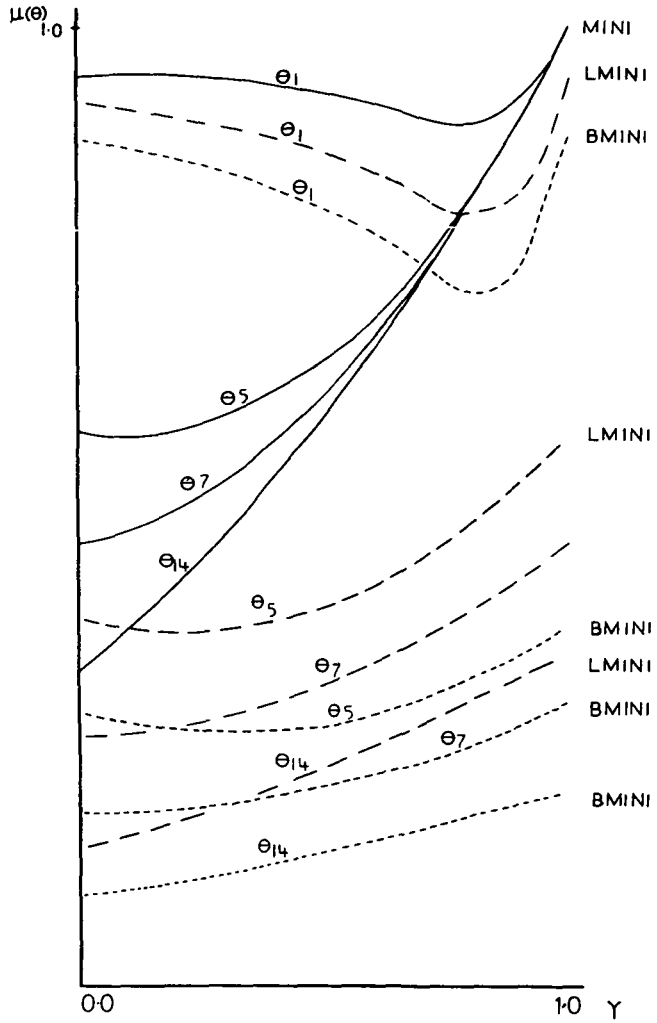

FIGURE 3. Smoothing factors for the two-dimensional Laplacian operator with MINI and LMINI. The smoothing factor for the three-dimensional Laplacian is shown for BMINI.

It is well known that blockings of the relaxation methods are more efficient, however, it is not immediately obvious (because of algebraic difficulties) that smoothing with the relaxation approach is superior with blocking for all ω and θ. Specific examples shown in Figure 4 suggests it is so for SOR and SLOR.

The block form of relaxation on a three-dimensional problem appears to have a greater potential for smoothing (over a significant portion of the ω range) than does either SLOR or SOR on a comparable two-dimensional problem. As the mesh becomes more tightly coupled and the value of ω selected increases, the smoothing terms move together for various frequencies.

https://doi.org/10.1017/S033427000000401X Published online by Cambridge University Press

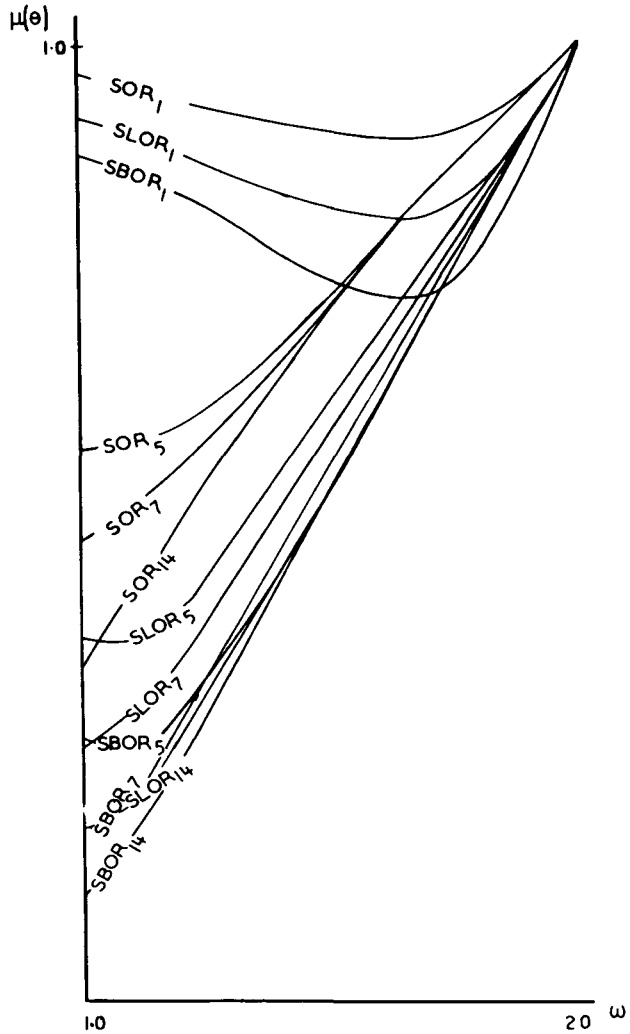

FIGURE 4. Smoothing factors for the two-dimensional Laplacian operator with SOR and SLOR. The smoothing factor for the three-dimensional Laplacian is shown for SBOR.

It also follows with the relaxation technique, that for ω somewhat greater than ω_{opt}, there appears to be only a small difference in the smoothing factor predicted by local mode analysis. This is related to SOR theory, where all eigenvalues of the iterative process become equal in absolute value for $\omega \geqslant \omega_{opt}$.

The maximum smoothing, predicted with local mode analysis for the low frequency components in Figure 4, coincides with the value of ω obtained by theory for SOR, and is not far from it for SLOR. In Table 1, the optimal values

https://doi.org/10.1017/S033427000000401X Published online by Cambridge University Press

Grid size n x n n	SOR		SLOR	
	ω_{opt} theory	ω_{opt} local mode	ω_{opt} theory	ω_{opt} local mode
4	1.23	1.26	1.03	1.15
8	1.48	1.49	1.27	1.36
16	1.69	1.69	1.55	1.60
32	1.82	1.82	1.75	1.76
64	1.91	1.91	1.86	1.87
128	1.95	1.95	1.93	1.93

TABLE 1. ω_{opt} evaluated from theory and predicted from a local mode analysis of lowest frequency components of error

of ω given by theory and predicted through the local model analysis are displayed for various grid subdivisions.

A 'local mode' examination of the block form of MINI and the relaxation techniques on three-dimensional problems, confirms that these methods have their work distributed between iterating in the (z) direction and in the block (x, y) planes. The analysis, in general, suggests that BMINI has a greater ability to smooth in the (z) direction than SBOR. The calculation of some large three-dimensional reactor models (Barry and Pollard [4] and Barry [5]) confirm this prediction. The Incomplete Choleski Conjugate Gradient (ICCG) technique has some potential for reactor studies, however, it is not a block form. Because the block forms (BMINI and SBOR) have to work harder than ICCG to converge the (x, y) plane, it is anticipated there might be a tradeoff against ICCG in the third dimension. The results referred to above support this suggestion. Unfortunately, it is difficult to extend the 'local mode' approach to handle the conjugate gradient method or any of its more recent variations.

Comparison of the smoothing factors (2.12) and (2.15) is an inadequate measure of the effectiveness of the two separate MINI processes for the three-dimensional calculations, because MINI in the (z) direction perturbs the diagonal terms of the (x, y) plane MINI matrix. The modified smoothing factor for the inner MINI process (based on this method) is

$$\mu^{\mathrm{MOD}}_{\mathrm{LMINI}}(\theta_1, \theta_2) = \frac{|be^{i\theta_2} - b\gamma_y|}{|2a + 2b + 2c - c\gamma_z - b\gamma_y - ae^{i\theta_1} - ae^{-i\theta_1} - be^{-i\theta_2}|}.$$

A comparison of $\mu^{\mathrm{MOD}}_{\mathrm{LMINI}}(\theta_1, \theta_2)$ and $\mu_{\mathrm{BMINI}}(\theta_1, \theta_2, \theta_3)$ with $(\gamma_z = \gamma_y)$ and $(a = b = c)$, for convenience, suggests that MINI in the (z) direction will remove higher

https://doi.org/10.1017/S033427000000401X Published online by Cambridge University Press

frequency components faster than the inner plane MINI iterative process, and that it may have trouble with the lower frequencies for certain γs.

The modified smoothing factor for the inner relaxation step is obtained similarly for this situation

$$\mu_{\mathrm{SLOR}}^{\mathrm{MOD}}(\theta_1, \theta_2) = \frac{\left|ap\left[e^{i\theta_1} - 2 + e^{-i\theta_1}\right] + be^{i\theta_2} - 2bp - 2cp\right|}{\left|\frac{a}{\omega}\left[e^{i\theta_1} - 2 + e^{-i\theta_1}\right] - \frac{2b}{\omega} - \frac{2c}{\omega} + be^{-i\theta_2}\right|}.$$

The 'local mode' Fourier analysis of the many relaxation techniques supports the hypothesis that their performances are limited by an inability to remove low frequency error components as rapidly as higher terms, for suboptimal estimates of ω_{opt}. Owing to difficulties in obtaining a precise determination of ω_{opt}, the performance of relaxation schemes may be enhanced (for low estimates) by a method which removes low order error components. The Jacobi scheme, as noted by Nicolaides [15] is an exception to the above observation; however, a weighted Jacobi technique is appropriate for a multigrid algorithm.

The 'local mode' analysis for MINI is more clear cut; for all γ, there is a general inability to cope with low frequency error relative to the higher frequencies.

Because the Fourier analysis is local in concept and does not accommodate boundary conditions, any interpretation of the results should be qualified accordingly!

In spite of these limitations the local mode analysis suggests MINI is a most likely candidate to benefit from coarse mesh rebalancing, because of the greater relative difficulty it has in suppressing the low frequency error components. The same conclusion cannot be drawn for successive overrelaxation techniques when accurate estimates of ω_{opt} are available. Experience over the years with relaxation methods for practical reactor configurations, however, has shown that, when CMR is applied, computational effort is considerably reduced. The benefit most likely arises either from a reduction in low frequency error components (when a suboptimal approximation to ω_{opt} is used), or simply from the better approximation to the true solution produced by CMR.

In an attempt to overcome criticism levelled at conclusions drawn from the localised study, recourse is made to Fourier transforms to permit a 'global' study of the frequency approach to convergence.

3. A global mode Fourier analysis of iterative methods

To investigate, in a global sense, the effect of the various iterative schemes on high frequency error components, the fast Fourier transform (Brigham [7]) is used

https://doi.org/10.1017/S033427000000401X Published online by Cambridge University Press

to determine the Fourier coefficients of the error vector at various stages of the iterative process. For this work, the subroutine DHARM (IBM [9]) is used in a two-dimensional mode to obtain the inverse series

$$A(k_1, k_2) = \frac{1}{N_1 N_2} \sum_{j_1=0}^{N_1-1} \sum_{j_2=0}^{N_2-1} X(j_1, j_2) e^{-2\pi i(j_1 k_1/N_1 + j_2 k_2/N_2)},$$

where $X(j_1, j_2)$ denotes the error component of the trial vector at the (j_1, j_2)th mesh point.

Two sample problems are analysed by the Fourier expansion. The first problem is

$$-\nabla^2 u(x, y) = f(x, y), \tag{3.1}$$

where the boundary condition $u = 0$ is applied on all sides of a square region, of side π. The right-hand side is computed from a solution $u(x, y) = \sin x \sin y$ over an equally spaced five-point finite difference approximation, used on 17×17 grid which includes the boundaries. A trial solution

$$u_0(x, y) = u(x, y) + \sum_{k=1}^{15} \sin kx \sin ky$$

was selected because it represents a wide selection of error frequencies of the same magnitude. A second problem

$$-\nabla^2 u(x, y) + \sigma(x, y) u(x, y) = f(x, y)$$

was selected, subject to the same boundary conditions and trial solution. The right-hand side $f(x, y)$ is calculated numerically to conform to the solution $u(x, y) = \sin x \sin y$, and $\sigma(x, y)$ is a function (equivalent to a neutron loss for the reactor physics problem) returning a random value in the range (0, 1).

Results are shown in Tables 2 and 3 after one, three, five and seven iterative steps with the four schemes MINI, ICCG, SLOR and Gauss-Seidel (GS). For MINI, the γs are redetermined continuously by the algorithm described in Barry and Pollard [2]. On the first MINI pass, a Gauss-Seidel iteration is used to commence the process. For SLOR, the optimal relaxation factor is used from the start. This is done because a numerical estimate of ω_{opt} may not have been obtained by the seventh iteration, and by then the GS process would have reduced the error too much for the purposes of comparison. Although ω may be obtained directly for problem 1, a numerical estimate (Pollard [17]) obtained from separate calculations is used in both problems.

https://doi.org/10.1017/S033427000000401X Published online by Cambridge University Press

Iterative Method	Iteration Count	E_M	E_A	FF (0,2)	FF (3,4)	FF (5,6)	FF (7,7)
MINI	1	2.83	0.457	0.48	0.23	0.18	0.11
	3	0.977	0.353	0.76	0.13	0.07	0.03
	5	0.609	0.248	0.80	0.11	0.06	0.02
	7	0.397	0.146	0.82	0.10	0.06	0.02
ICCG	1	1.31	0.413	0.57	0.21	0.13	0.09
	3	0.597	0.277	0.77	0.14	0.06	0.03
	5	0.401	0.183	0.79	0.13	0.05	0.02
	7	0.266	0.119	0.80	0.13	0.05	0.02
SLOR	1	5.02	0.602	0.26	0.24	0.30	0.20
	3	2.53	0.390	0.26	0.25	0.29	0.20
	5	1.09	0.183	0.27	0.24	0.29	0.20
	7	0.436	0.087	0.27	0.23	0.30	0.20
GS	1	2.83	0.457	0.48	0.23	0.18	0.11
	3	1.06	0.375	0.79	0.12	0.06	0.03
	5	0.770	0.318	0.85	0.09	0.05	0.02
	7	0.625	0.272	0.85	0.08	0.05	0.02

TABLE 2. A Fourier analysis of four iterative schemes for problem 1

To assist the interpretation of an otherwise massive number of Fourier coefficients in the error expansion

$$v(j_1, j_2) = \sum_{k_1=0}^{15} \sum_{k_2=0}^{15} A_{k_1 k_2} e^{2\pi i(j_1 k_1/16 + j_2 k_2/16)} \quad \begin{cases} 0 \leqslant j_1 \leqslant 15, \\ 0 \leqslant j_2 \leqslant 15, \end{cases}$$

the Fourier coefficients $A_{k_1 k_2}$ are grouped and analysed by range. The range (n_1, n_2) is defined to include all terms whose indices k_1 and k_2 satisfy

$$n_1 \leqslant k_1 \leqslant n_2 \quad \text{for } 0 \leqslant k_2 \leqslant n_2$$

and

$$n_1 \leqslant k_2 \leqslant n_2 \quad \text{for } 0 \leqslant k_1 \leqslant n_1.$$

https://doi.org/10.1017/S033427000000401X Published online by Cambridge University Press

Iterative Method	Iteration Count	E_M	E_A	FF (0,2)	FF (3,4)	FF (5,6)	FF (7,7)
MINI	1	2.59	0.320	0.44	0.25	0.20	0.11
	3	0.423	0.093	0.69	0.17	0.10	0.04
	5	0.090	0.010	0.67	0.18	0.10	0.04
	7	0.030	0.003	0.60	0.24	0.11	0.05
ICCG	1	0.989	0.222	0.50	0.24	0.15	0.11
	3	0.103	0.030	0.55	0.28	0.13	0.04
	5	0.013	0.004	0.56	0.28	0.12	0.04
	7	0.002	0.0005	0.57	0.28	0.11	0.04
SLOR	1	3.28	0.299	0.29	0.24	0.28	0.19
	3	0.422	0.064	0.36	0.21	0.25	0.18
	5	0.070	0.010	0.44	0.20	0.21	0.14
	7	0.010	0.002	0.49	0.20	0.18	0.12
GS	1	2.59	0.320	0.44	0.25	0.20	0.11
	3	0.533	0.125	0.71	0.16	0.09	0.04
	5	0.188	0.051	0.78	0.10	0.08	0.04
	7	0.070	0.020	0.76	0.12	0.08	0.04

TABLE 3. A Fourier analysis of four iterative schemes for problem 2

The fraction that all Fourier coefficients in the range (n_1, n_2) form of all the Fourier components after an iterative step is shown as $FF(n_1, n_2)$, *i.e.*

$$FF(n_1, n_2) = \frac{\Sigma_{k_1}\Sigma_{k_2}|\bar{A}_{k_1k_2}|}{\Sigma_{l_1=0}^{15}\Sigma_{l_2=0}^{15}|\bar{A}_{l_1l_2}|}, \tag{3.2}$$

where unspecified summation is taken to be over the range (n_1, n_2). The maximum variation between iterations $E_M = \max|u_{ij}^{(n+1)} - u_{ij}^{(n)}|$ and average variation $E_A = \Sigma_{i=0}^{15}\Sigma_{j=0}^{15}|u_{ij}^{(n+1)} - u_{ij}^{(n)}|/256$ are reported also.

The error in the initial estimate has a wide distribution of error components across the frequency spectrum. Consideration of $FF(n_1, n_2)$ reveals a significant shift in the proportion of frequency terms that comprise the new error after even one iteration with MINI (= GS), and ICCG. After three iterations for both problems considered, the proportion of the various frequency terms comprising

https://doi.org/10.1017/S033427000000401X Published online by Cambridge University Press

the error stabilises, the high frequency components being almost insignificant. For problem 1 with SLOR, the distribution of frequency components remains fairly static, while for problem 2, a small relative decrease in the contribution made by the high frequency error components is observed. This is in keeping with the theoretical understanding and expectations of SLOR. In problem 1, the error components belong to the set of eigenvectors of the associated Jacobi iterative matrix, and these eigenvalues have a reasonably uniform distribution. A selection of $\omega = \omega_{opt}$ ensures that all the eigenvalues of the iteration matrix are transformed to lie on the complex circle of radius $\omega - 1$ (Young [21]). Even if small errors occur in the estimate of ω_{opt}, the distribution of Jacobi eigenvalues is such that most, if not all, the transformed eigenvalues still fall on the circle.

When ω_{opt} is known exactly, the eigenvalues of the iterative scheme are identical in magnitude. This is confirmed in problem 1 and it seems pointless to search for a scheme which facilitates removal of low frequency error alone. A Fourier study involving a 10 per cent lower estimate of ω_{opt}, however, reveals a difference in the relative rate of error reduction.

For problem 2, a more selective elimination of frequency components is achieved through the iterative process. For less straightforward iterative matrices than those of problem 1, eigenvalues may cluster and errors in the precise determination of ω_{opt} may affect the number of eigenvalues which are transformed to lie on the circle. This in turn will influence the relative decay rate of the Fourier terms. Under these circumstances, consideration of coarse mesh rebalancing techniques may be worthwhile. Reactor physicists traditionally have benefited from accelerating SLOR with rebalance techniques.

4. Coarse mesh rebalancing (CMR)

The iterative solution for the $N \times N$ linear system $A\mathbf{x} = \mathbf{b}$, arising from a finite difference, or finite element, discretisation of a continuous problem is accelerated by imposing a coarse $K \times K$ grid over the fine grid. Starting with an initial estimate $\mathbf{x}_0$ of $\mathbf{x}$, a new estimate $\mathbf{x}$ is sought such that

$$\mathbf{x}_1 = f(\mathbf{x}_0, P, \mathbf{c}),$$

where $\mathbf{x}$ is computed so as to minimise the residual $\mathbf{r} = A\mathbf{x} - \mathbf{b}$. The precise definition of f, P and $\mathbf{c}$ depends upon the particular form of CMR. Here, P is a matrix operator which partitions the fine mesh into a coarse mesh structure while the components of $\mathbf{c}$ are determined by the weighted residual method of Nakamura [14]. (The number of elements of $\mathbf{c}$ varies with the type of CMR, but is proportional to K^2.) The positioning of the coarse mesh grid points relative to the fine mesh points depends upon the type of partitioning.

https://doi.org/10.1017/S033427000000401X Published online by Cambridge University Press

A discrete Fourier analysis is performed on four coarse mesh rebalance schemes of the nuclear code POW3D for two sample problems. Results for the two test problems are reported in Tables 4 and 5. The first problem and its boundary conditions are as given by (3.1), where the right-hand side is calculated numerically for a solution $U^1(x, y) = (\pi - x)(\pi - y)xy$ over a 17×17 grid which includes the boundaries. For the second problem a solution $U^2(x, y) = \sin x \sin y$ is selected and the right-hand side evaluated similarly.

For the first example, the trial solution $U_0^1(x, y) = U^1(x, y) + \sin x \sin y$ is used, while for the second $U_0^2(x, y) = U^2(x, y) + (\pi - x)(\pi - y)xy$ is employed. Both trial estimates were chosen because the error involved is not fluctuating rapidly. Care was taken to avoid an error component that is an exact multiple of the solution itself, because the multiplicative schemes completely remove the error from the trial solution under these circumstances (Barry [5]).

For the rebalancing operation, the coarse grid imposed on the 17×17 fine mesh satisfied the following criteria for the four methods analysed:

(i) the order of the reduced system of linear equations is the same for each method,

(ii) the number of coarse mesh points for each axis is approximately the square root of the number of fine mesh points (5 and 4 for the disjunctive and pyramid partitioning methods respectively),

(iii) the coarse mesh points are positioned as symmetrically as possible.

The error vector before and after rebalancing is analysed by the fast Fourier inverse transform. This time the reported quantity $FF(n_1, n_2)$ defined previously by (3.2) is the fraction that all Fourier coefficients in the range (n_1, n_2) form of all the Fourier coefficients of error after application of the coarse mesh rebalance procedure.

It is worth reporting two additional parameters. The first is represented by $FR(n_1, n_2)$ and is the fraction (of the original error) to which all the diminished Fourier components in the range (n_1, n_2) are reduced, *i.e.*,

$$FR(n_1, n_2) = 1 - \frac{\Sigma_{k_1} \Sigma_{k_2} \left| \left(|A_{k_1 k_2}| - |\bar{A}_{k_1 k_2}| \right) \right|}{\Sigma_{k_1} \Sigma_{k_2} |A_{k_1 k_2}|} \quad \text{for all } \frac{|\bar{A}_{k_1 k_2}|}{|A_{k_1 k_2}|} \leqslant 1,$$

where the unspecified summation is again over the range (n_1, n_2), and where $A_{k_1 k_2}$ and $\bar{A}_{k_1 k_2}$ represent the Fourier coefficients before and after rebalancing respectively. (A small value of FR indicates considerable reduction in the error component.) The final quantity is the proportion of all terms within a range (n_1, n_2) which are reduced by CMR, and this is expressed as a percentage.

The four CMR methods tested are:

Method 1. Multiplicative disjunctive partitioning-disjunctive weighting.

https://doi.org/10.1017/S033427000000401X Published online by Cambridge University Press

The rebalanced vector $\mathbf{x}_1$, is given by

$$\mathbf{x}_1 = \sum_{k=1}^{(K-1)^2} (c_k P_k)\mathbf{x}_0.$$

The $N \times N$ diagonal matrices P_k satisfy

(i)

$$\operatorname{diag}(P_k)_l \begin{cases} = 1 \text{ for all points in the } k\text{th coarse mesh partition} \\ = 0 \text{ otherwise, and} \end{cases}$$

$$\sum_{k=1}^{(K-1)^2} P_k = I.$$

(ii) The coarse mesh grid points lie between fine mesh points (Figure 5). The $(K-1)^2$ disjunctive weighting vectors (of length N^2) are given by $\mathbf{w}_k = P_k\mathbf{1}$, where $\mathbf{1}$ is a vector of length N^2 with unit components. The parameters c_k satisfy the $(K-1)^2$ inner product linear system

$$\sum_{k=1}^{(K-1)^2} \langle \mathbf{w}_l, AP_k\mathbf{x}_0 \rangle c_k = \langle \mathbf{w}_l, \mathbf{b} \rangle \qquad \left(l = 1, 2, \ldots, (K-1)^2\right).$$

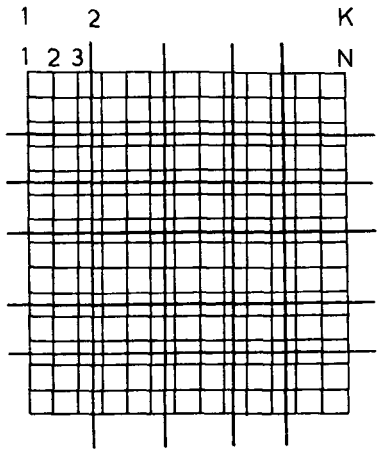

FIGURE 5. Coarse grid for disjunctive partitioning.

Method 2. Multiplicative pyramid partitioning-disjunctive weighting.

The elements of P_k are defined by bilinear functions which are of unit height at the kth coarse mesh grid point and zero on the boundaries of the surrounding rectangular coarse grid. The coarse grid points this time actually coincide with fine mesh grid points (Figure 6). The corrected vector $\mathbf{x}_1$, is given by

$$\mathbf{x}_1 = \sum_{k=1}^{K^2} (c_k P_k)\mathbf{x}_0,$$

https://doi.org/10.1017/S033427000000401X Published online by Cambridge University Press

while elements of the K^2 weighting functions used for the weighted residual method are defined to be unity if the corresponding diagonal component of P_k is non-zero, and zero otherwise.

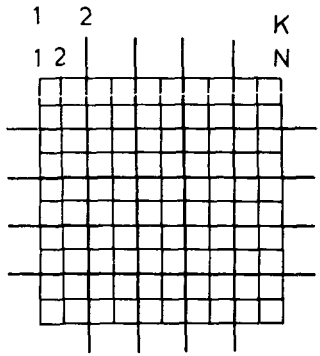

FIGURE 6. Coarse grid for pyramid partitioning.

Method 3. Additive pyramid partitioning-disjunctive weighting.

The rebalanced vector $\mathbf{x}_1$, is given by

$$\mathbf{x}_1 = \mathbf{x}_0 + \sum_{k=1}^{K^2} c_k \operatorname{diag}(P_k),$$

where the P_k and $\mathbf{w}_k$ are as defined for Method 2, but the weighted residual scheme requires solution of the system of K^2 linear equations

$$\sum_{k=1}^{K^2} \langle \mathbf{w}_l, A \operatorname{diag}(P_k) \rangle c_k = \langle \mathbf{w}_l, \mathbf{b} - A\mathbf{x}_0 \rangle \qquad (l = 1, 2, \ldots, K^2).$$

Method 4. Additive pyramid partitioning-Galerkin weighting.

This is the same as Method 3, except for Galerkin weighting.

The disjunctive method is a variation of that proposed first by Wachspress [20], while the other three are more recent, influenced perhaps by developments in finite element applications. Nakamura [14] gives a more detailed description and refers to other possible schemes as well.

Of the three methods involving non-Galerkin weighting, the multiplicative pyramid and disjunctive partitioning schemes show a significant reduction in the error of the estimate after CMR is applied. There appears to be a very significant reduction of error in the low frequency groups as indicated by $FR(0, 2)$. For these two methods every individual Fourier component was reduced.

https://doi.org/10.1017/S033427000000401X Published online by Cambridge University Press

Method of CMR	E_M	E_A	FF (0,2)	FF (3,4)	FF (5,6)	FF (7,7)	FR (0,2)	FR (3,4)	FR (5,6)	FR (7,7)	% of terms reduced (0,2)	% of terms reduced (3,4)	% of terms reduced (5,6)	% of terms reduced (7,7)
Disjunctive partitioning	0.13	0.04	0.81	0.09	0.07	0.03	0.11	0.12	0.17	0.17	100	100	100	100
Multiplicative pyramid partitioning	0.06	0.03	0.77	0.13	0.06	0.04	0.06	0.11	0.09	0.14	100	100	100	100
Additive pyramid partitioning	0.67	0.30	0.79	0.11	0.05	0.04	0.63	0.73	0.36	0.98	44	56	63	13
Additive pyramid partitioning	0.24	0.04	0.67	0.17	0.10	0.05	0.18	0.50	0.52	0.59	100	100	92	67
Galerkin weighting														

TABLE 4. Fourier analysis of CMR for $u = (\pi - x)(\pi - y)xy$ with $u_0 = u + \sin(x)\sin(y)$.

Method of CMR	E_M	E_A	FF (0,2)	FF (3,4)	FF (5,6)	FF (7,7)	FR (0,2)	FR (3,4)	FR (5,6)	FR (7,7)	% of terms reduced (0,2)	% of terms reduced (3,4)	% of terms reduced (5,6)	% of terms reduced (7,7)
Disjunctive partitioning	0.13	0.04	0.81	0.09	0.07	0.03	0.02	0.02	0.02	0.02	100	100	100	100
Multiplicative pyramid partitioning	0.06	0.03	0.77	0.13	0.06	0.04	0.01	0.01	0.01	0.02	100	100	100	100
Additive pyramid partitioning	4.35	1.99	0.78	0.11	0.06	0.05	0.70	0.63	0.47	0.81	89	56	63	13
Additive pyramid partitioning Galerkin weighting	1.19	0.27	0.61	0.22	0.11	0.06	0.14	0.44	0.36	0.49	100	100	100	93

TABLE 5. Fourier analysis of CMR for $u = \sin(x)\sin(y)$ with $u_0 = u + (\pi - x)(\pi - y)xy$.

Method of CMR	E_M	E_A	FF (0,2)	FF (3,4)	FF (5,6)	FF (7,7)	FR (0,2)	FR (3,4)	FR (5,6)	FR (7,7)	% of terms reduced (0,2)	% of terms reduced (3,4)	% of terms reduced (5,6)	% of terms reduced (7,7)
Multiplicative pyramid partitioning	0.08	0.03	0.77	0.12	0.08	0.03	0.06	0.11	0.13	0.11	100	100	100	100
Additive pyramid partitioning	0.80	0.03	0.77	0.12	0.08	0.02	0.11	-	-	-	89	0	0	0
Additive pyramid partitioning Galerkin weighting	0.09	0.02	0.40	0.38	0.13	0.10	0.06	0.59	0.35	0.63	100	100	100	100

TABLE 6. Fourier analysis of CMR for $u = (\pi - x)(\pi - y)xy$ with $u_0 = u + \sin(x)\sin(y)$ with a coarse mesh expected to favour the additive schemes (– indicates no reduction obtained).

The high values of *FF* reported for the low frequency components may appear to be disappointing at first sight. They are a little misleading on their own and this is why the second quantity *FR* was computed subsequently. The value of *FF* is high for low frequency terms, simply because the original error in the approximate solution is made up of predominantly low frequency components itself. After the rebalance, the error still has a high relative proportion of the low frequency terms even though they are reduced absolutely in magnitude (a fact reflected in *FR*). To some extent, a high value of *FF* indicates that the rebalance process does not have a significant parasitic effect of exciting high frequency error components in these examples.

The reduction in the error is not restricted to the low end of the spectrum (as indicated by *FR*). The non-linear multiplicative nature of the schemes allows for this, whereas the same effect is less likely with simpler mapping operations between coarse and fine grids. This is verified by the two additive forms, where the value of *FR* for the high frequency terms is significantly higher.

The additive pyramid approach without Galerkin weighting seems of little value compared with the other three procedures. In fact, many of the Fourier coefficients are increased by this rebalancing.

Significant improvement occurs for the additive method if Galerkin weighting vectors are selected instead of disjunctive weights. Almost all the Fourier terms are reduced, and a marked reduction in low frequency terms (relative to the higher frequencies) is observed for the two examples. Such vectors, however, require additional computation.

The location of the 4×4 coarse grid system achieved by the criteria above for the pyramid partitioning is not as favourable to the additive forms of rebalance, because the point $(\pi/2, \pi/2)$ at which the error is a maximum is not a coarse mesh grid point. An alternative coarse mesh grid that exploited this knowledge overcame the seemingly high maximum and average error reported for sample problems with additive rebalance (provided Galerkin weighting was used). The results with the newer coarse grid mesh for the first problem with three of the CMR routines are presented in Table 6. The results indicate little change for the very satisfactory multiplicative pyramid form, even though additional coarse mesh lines are introduced to pass through $(\pi/2, \pi/2)$. The additive form involving Galerkin weighting showed a dramatic improvement which made it comparable to the multiplicative pyramid form. The multiplicative forms seem less sensitive to the positioning of the coarse grid for the class of problems considered. This undoubtedly is due to the multiplicative nature of the rescaling process. For the pyramid form there is an effective increase in the polynomial order of the approximation. Despite their better performance, there is considerably more computational overhead in employing the multiplicative schemes.

When the initial estimate is

$$U_0(x, y) = (\pi - x)(\pi - y)xy + e$$

where $e = \sin kx \sin ky$, the coarse mesh rebalance no longer shows the same improvement as k increases. Once k exceeds the order of the coarse mesh grid, application of CMR actually increases the error in the solution estimate. A good computational strategy, where the error is known to be highly oscillatory, is to undertake a few ordinary iterations on the fine grid to remove much of the high frequency spectrum and then apply CMR. The findings suggested by Tables 4 and 5 are supported in general by many other examples when subjected to the same analysis. It is possible to choose error components where the additive approach is advantaged; however, actual reactor computations performed to date with POW3D indicate superior performance with multiplicative forms.

5. Conclusions

Despite certain limitations of the 'local mode' approach, it provides some interesting insights into the removal of error components with the iterative approaches. These insights are supported by the more conventional 'global' approach. Predictions from 'local mode' analysis do not contradict well-established results for the relaxation methods.

In addition, the Fourier approach suggests the MINI technique will converge provided $0 \leqslant \gamma < 1$. Practical experience has demonstrated the need for an upper limit of unity; however, a theoretical investigation based on the approaches adopted for relaxation methods (Varga [19]), has so far, only guaranteed convergence for the range $0 \leqslant \gamma < 1/2$.

The conjugate gradient and MINI iterative schemes appear to be well suited to the rapid removal of high frequency error components. Each of them seems an ideal candidate for use with the secondary acceleration provided by the low frequency error removal from CMR.

References

[1] J. M. Barry, B. V. Harrington and J. P. Pollard, "POW3D", *Austral. Atomic Energy Commission Report E series* (to appear).

[2] J. M. Barry and J. P. Pollard, "Method of implicit nonstationary iteration for solving neutron diffusion linear equations", *Ann. Nuclear Energy* 4 (1977), 485–493.

[3] J. M. Barry and J. P. Pollard, "Application of the method of implicit non-stationary iteration (MINI) to 3D neutron diffusion problems", *Ann. Nuclear Energy* 6 (1979), 121–131.

[4] J. M. Barry and J. P. Pollard, "Solution of neutron diffusion linear equations by the method of implicit nonstationary iteration", in *Numerical solutions of partial differential equations* (ed. J. Noye), (North-Holland, 1982), 605–622.
[5] J. M. Barry, "Multi-dimensional neutron diffusion", Ph.D. Thesis, Wollongong University, 1982.
[6] A. Brandt, "Multi-level adaptive solutions to boundary-value problems", *Math. Comp.* 31 (1977), 333–390.
[7] E. O. Brigham, *The fast Fourier transform* (Prentice Hall, 1974).
[8] G. Doherty, private communication.
[9] IBM, "System/360 Scientific Subroutine Package Version III", GH20-0205-4, (1970).
[10] J. A. Meijerink and H. A. van der Vorst, "An iterative solution method for linear systems of which the coefficient matrix is a symmetric M-matrix", *Math. Comp.* 31 (1977), 148–162.
[11] S. Nakamura, "A variational rebalancing method for linear iterative convergence scheme of neutron diffusion and transport equations", *Nuclear Sci. Engrg.* 39 (1970), 278–283.
[12] S. Nakamura, "Coarse mesh acceleration of iterative solution of neutron diffusion equations", *Nuclear Sci. Engrg.* 43 (1971), 116–120.
[13] S. Nakamura, "Analysis of coarse mesh rebalancing effect", *Nuclear Sci. Engrg.* 61 (1976), 98–106.
[14] S. Nakamura, *Computational methods in engineering and science* (Wiley, 1977).
[15] R. A. Nicolaides, "On multiple grid and related techniques for solving discrete elliptic systems", *J. Comput. Phys.* 19 (1975), 418–431.
[16] J. P. Pollard, 'Subroutine SOK-iterative solution of linear equations by the method of averaging functional corrections', *Austral. Atomic Energy Commission Report E*192, (1968).
[17] J. P. Pollard, "Numerical methods used in neutronics calculations", Ph.D. Thesis, University of New South Wales, 1973.
[18] J. K. Reid, "On the method of conjugate gradients for the solution of large sparse systems of linear equations", in *Large sparse sets of linear equations* (ed. J. K. Reid), (Academic Press, 1971), 231–254.
[19] R. S. Varga, *Matrix iterative analysis* (Prentice-Hall, 1962).
[20] E. L. Wachspress, *Iterative solution of elliptic systems* (Prentice-Hall, 1966).
[21] D. M. Young, *Iterative solution of large linear systems* (Academic Press, 1971).